

XNNT_{AB}– Interpretable Neural Networks for Tabular Data using Sparse Autoencoders

Khawla Elhadri^[0009–0008–2696–8331], Jörg Schlötterer^[0000–0002–3678–0390], and Christin Seifert^[0000–0002–6776–3868]

Marburg University, Germany

khawla.elhadri@uni-marburg.de, joerg.schloetterer@uni-marburg.de,
christin.seifert@uni-marburg.de

Abstract. In data-driven applications relying on tabular data, where interpretability is key, machine learning models such as decision trees and linear regression are applied. Although neural networks can provide higher predictive performance, they are not used because of their blackbox nature. In this work, we present XNNT_{AB}, a neural architecture that combines the expressiveness of neural networks and interpretability. XNNT_{AB} first learns highly non-linear feature representations, which are decomposed into monosemantic features using a sparse autoencoder (SAE). These features are then assigned human-interpretable concepts, making the overall model prediction intrinsically interpretable. XNNT_{AB} outperforms interpretable predictive models, and achieves comparable performance to its non-interpretable counterparts. The code is available at <https://github.com/ke-pm/XNNTAB>.

Keywords: Deep Neural Networks · Tabular Data · Interpretable Models.

1 Introduction

Tabular data is the most common type of data in a wide range of industries, including advertising, finance and healthcare. While deep neural networks (DNNs) achieved major advances in computer vision, their performance on tabular data remained below that of Gradient Boosted Decision Trees (GBDTs) [5, 16]. To improve the performance of DNNs on tabular data, several deep learning methods have been developed with specialized architectures that take into account the unique traits of tabular data (mixture of categorical, ordinal and continuous features) in order to be on par [12] or even outperform GBDTs [4]. While these methods address the limitations of DNNs in terms of performance, DNNs still remain blackboxes, whose decisions are hard to communicate to end users [21].

In this paper, we address the interpretability limitations of existing DNNs and introduce XNNT_{AB}¹, a deep neural network incorporating a sparse autoencoder (SAE). The SAE learns a dictionary of monosemantic, sparse features, and XNNT_{AB} uses only these monosemantic features to generate outcome predictions, ensuring intrinsic interpretability. We take inspiration from the success of SAEs in learning interpretable

¹ The research in this paper was presented in a early stage at UniReps: 3rd Edition of the Workshop on Unifying Representations in Neural Models at NeuRIPS 2025 [7]

features from LLM’s internal activations [13, 25], and assume that monosemanticity holds for tabular data. While LLMs are used to explain the learned features in NLP, we use an automated rule based method to assign human-understandable semantics to the learned dictionary features. Our method is illustrated in Figure 1 and described in Section 3. We show that XNNT_{AB} outperforms interpretable models and matches the performance of blackbox models. XNNT_{AB} is fully interpretable: the final prediction is a simple linear combination of dictionary features with clear human-understandable semantics.

2 Related Work

Gradient boosted decision trees (GBDTs) [5, 16] have shown state-of-the art performance on tabular data [11], outperforming standard neural architectures. To close this performance gap, neural architectures specifically tailored to tabular data have been proposed, such as attention-based architectures [10, 23, 24], and retrieval-augmented models [9, 23]. Further approaches include regularizations [14], deep ensembles [8], attentive feature selection [2], feature embeddings [12], and reconstruction of binned feature indices [18].

Recent methods focus not only on performance, but also aim to include interpretability. ProtoGate [15] is an ante-hoc interpretable architecture for tabular data, which learns prototypes of classes and predicts new instances based on their similarity to class prototypes. InterpretTabNet [22], a variant of TabNet [2] adds post-hoc explanations by learning sparse feature attribution masks and using LLMs to interpret the learned features from the masks. Similar to ProtoGate and different from InterpretTabNet, XNNT_{AB} is intrinsically interpretable, i.e., it uses interpretable features directly for prediction. While ProtoGate relies on class prototypes, XNNT_{AB} learns relevant feature combinations that describe parts of instances, similar to part-prototype models [6].

3 XNNT_{AB}

XNNT_{AB} consists of a standard neural blackbox (e.g., an MLP) to learn nonlinear latent features, and a sparse autoencoder (SAE) [13] to decompose this latent polysemantic feature space into monosemantic features (cf. Figure 1, A). The monosemantic features are in a latent space with unknown (but unique) semantics. To assign meaning to each feature, we learn rules that describe the subset of the training samples that highly activate each feature (cf. Figure 1, B). Finally, we combine the last linear layers into a single linear layer by multiplying their weight matrices (cf. Figure 1, C), making the final prediction a direct linear combination of the monosemantic, rule-defined features..

3.1 Architecture

The base blackbox model is an MLP with multiple hidden layers and a softmax output. We denote the penultimate layer as l , and the representations of this layer as h_l . The MLP learns a function $\hat{y} = f(x)$. $f(x)$ can be decomposed into a function g learning

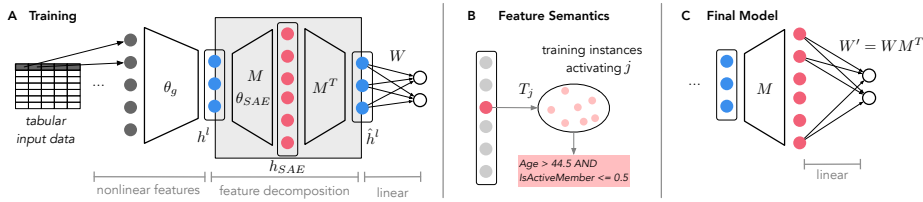


Fig. 1: Architecture overview. **A.** An MLP learns nonlinear features, which are decomposed into monosemantic dictionary features using an SAE. **B.** Dictionary features are assigned a human-interpretable meaning by learning rules for the subset of training instances that highly activate a specific feature. **C.** Predictions are linear combinations of monosemantic features by combining the linear model components (the decoder, M^T , and the linear layer of the MLP, W).

the hidden representations h_l and a linear model h predicting the target based on h_l , i.e., $\hat{y} = h(h_l) = h(g(x))$. $g(\cdot)$ is characterized by the parameters θ_g , and $h(\cdot)$ is characterized by the weight matrix W .

We adopt the SAE architecture described in [13], consisting of an input layer, a hidden layer, and an output layer. The weights of the encoder and decoder are shared, and given by the matrices M and M^T , respectively. The encoder has an additional bias vector b , the decoder has not [13]. We set the size of the hidden layer as $d_{hid} = R \cdot d_{in}$ with d_{in} being the dimension of the MLP’s layer l . R is a hyperparameter that controls the size of the feature dictionary. The input to the SAE are the hidden representations of the blackbox MLP h_l . The output of the SAE is given by $\hat{h}_l = M^T(\text{ReLU}(Mh_l + b))$. By design, \hat{h}_l is a sparse linear combination of (latent) monosemantic dictionary features [13].

3.2 Training

XNNTAB is trained in four steps: i) training of the MLP’s representation, ii) training of the SAE, iii) finetuning of the decision layer, and iv) combining linear components.

Step 1: MLP training. The MLP’s parameters $\theta_{MLP} = (\theta_g, W)$ are trained using cross-entropy loss and L1 regularization. The SAE is not present in this step.

Step 2: SAE Training. To learn a dictionary of monosemantic features we follow the training procedure of [13]. The SAE is trained to reconstruct the hidden activations h_l of training samples x . The SAE uses a reconstruction loss on its output and a sparsity loss on its hidden activations h_{SAE} to learn sparse dictionary features.

Step 3: Finetuning the decision layer. We freeze the parameters θ_g of the MLP and θ_{SAE} of the SAE and finetune the weights W in the decision layer with the same loss as in step 1 to make predictions from the reconstructions \hat{h}_l learned by the SAE.

Step 4: Aggregating linear components. Both, the decoder part of the SAE and the final decision layer of the MLP are linear layers, and can be combined into one layer. Therefore, we directly connect the hidden layer of the SAE to the output and set the weights of this layer to $W' = WM^T$.²

² $\hat{h}_l = M^T h_{SAE}$, and $\hat{y} = W\hat{h}_l = WM^T h_{SAE}$

Table 1: Dataset overview. Showing the number of instances, the number of numerical features (# Num.), the number of categorical features (# Cat.) and the machine learning task (Task).

Abbr	Name	Instances	# Num.	# Cat.	Task
AD	Adult	48,842	6	9	binary classification
CH	Churn Modeling	10,000	10	1	binary classification
CR	Credit_g	1,000	7	14	binary classification
SB	Spambase	4,601	57	1	binary classification
GE	Gesture	9,873	32	0	multi-class classification
CO	Covertypes	581,012	54	0	multi-class classification
CA	Car	1,728	0	7	multi-class classification

3.3 Learning Representation Semantics

The hidden representations of the SAE represent monosemantic dictionary features in a latent space, but their semantics are unknown. To assign human-understandable semantics to those features, we follow a similar idea as in [13] for tabular data instead of text (cf. Figure 1, B). For each dimension in the latent representation of the SAE $j \in \{1, \dots, d_{hid}\}$, we identify the subset of training samples T_j which highly activate this feature, i.e., whose activations are above a threshold p . We then use a rule-based classifier to learn simple decision rules describing this subset.

4 Experimental Setup

We train XNNTAB on 7 publicly available datasets, and compare the performance to interpretable models, classical blackbox models and state-of-the-art deep learning models.

4.1 Datasets and Evaluation Metrics

We evaluated XNNTAB on benchmark datasets for structured data from previous literature: Adult [17], Churn Modeling³, Spambase⁴, Credit_g⁵, Gesture Phase Prediction [19], Covertypes [3] and Car⁶. An overview of the datasets is shown in Table 1. We used 5-fold-cross-validation with 65%/15%/20% (training/validation/test) splits. We report macro F1 on the test set, averaged across all folds.

4.2 Models and Parameters

We compare XNNTAB to interpretable baselines, classical machine learning models and neural models, which are specifically designed for learning on tabular data.

³ <https://www.kaggle.com/shrutimechlearn/churn-modelling>

⁴ <https://openml.org/search?type=data&status=active&id=44>

⁵ <https://openml.org/search?type=data&status=active&id=31>

⁶ <https://openml.org/search?type=data&status=active&id=40975>

As baselines, we use two interpretable models, Logistic Regression (LR) and Decision Trees (DTs), and two blackbox models, XGBoost and Random Forests (RF). We further compare XNNTAB to recent deep learning models, namely TabNet [2], NODE [20], T2G-Former [24], FT-Transformer [10], TabM [8], TabR [9] and InterpreTabNet [22]. We report the experimental results of each model from their respective papers, TabNet and Node results are reported from T2G-Former. Note, that TabNet, NODE, T2G-Former, FT-Transformer, TabM, TabR and InterpreTabNet use a different training process: each dataset is split once into 65%/15%/20% (training/validation/test). After tuning hyperparameters on the validation set, 15 experiments are run with different random seeds, reporting average performance on the test set.

Our neural base model for XNNTAB is an MLP, with a different architecture for each dataset. We perform a neural architecture search on each cross-validation split and select the architecture with the smallest last hidden layer overall. We use the validation sets for tuning other hyperparameters using the Optuna library [1]. See Appendix A.2 for details on all hyperparameters.

4.3 Learning Representation Semantics

To assign human-understandable semantics to the dictionary features, we employ Skope-rules⁷. The Skope-rules classifier learns rule-based descriptions of a target subset by framing the task as binary classification: instances in the subset are labeled 1, all others 0. It outputs candidate rules along with their recall, each capturing different portions of the subset. If no suitable rule exists, it may return an empty rule set.

We identify the instances that most strongly activate each dictionary feature and use Skope-rules to describe these features. We use the default Skope-rules hyperparameters and set the precision to 1.0. Preliminary experiments showed that no single activation threshold yields rules for all features: some neurons never activate, some rarely activate and some produce no extractable rule at certain thresholds. However, all activated features are used for prediction. To obtain an optimal rule set for the dictionary features f_j , we therefore perform the following steps:

1. Pass the dataset through the model and record each neuron’s activation, yielding one activation value per instance.
2. For $p \in \{90\%, 80\%, 70\%, 60\%, 50\%\}$, select the top- p activations of neuron j and the corresponding instances, forming the subset T_j^p .
3. For each T_j^p , label its instances as 1 and all others as 0, run Skope-rules, and select the rule with the highest recall.
4. For each p , count how many dictionary features obtained a rule and choose the p that maximizes this count; break ties using the highest average recall.

5 Results

In this section, we report predictive performance, show qualitative and quantitative results on interpretability and analyze the impact of the activation threshold.

⁷ <https://github.com/scikit-learn-contrib/skope-rules>. Accessed July 2025

Table 2: Macro F1 of blackbox (×) and fully interpretable (✓) models on two benchmark datasets. Best values are marked bold, best values for interpretable models bold italic. The standard deviation for all experiments is small (max: 0.032, min: 0.001).

	AD ↑	CH ↑	CR ↑	SB ↑	CO ↑	GE ↑	CA ↑
× RF	0.799	0.747	0.657	0.947	0.838	0.596	0.908
× XGBoost	0.815	0.750	0.716	0.957	0.942	0.638	0.974
× MLP	0.796	0.751	0.693	0.945	0.870	0.632	0.955
✓ LR	0.782	0.601	0.701	0.921	0.476	0.224	0.358
✓ DTs	0.787	0.735	0.645	0.915	0.844	0.448	0.932
✓ XNNT _{AB}	0.795	0.752	0.700	0.948	0.878	0.634	0.955

5.1 Performance

Table 2 shows that, on nearly all datasets, XNNT_{AB} outperforms interpretable models, with the exception of CR, for which XNNT_{AB} is on par with Logistic Regression. On AD, XNNT_{AB} is comparable to MLP and slightly below the performance of XGBoost and Random Forest. On CH and GE, XNNT_{AB} is on par with all baseline blackbox models including XGBoost. On CR, SB and CO, XNNT_{AB} outperforms MLP and is slightly below XGBoost. These results show that our model introduces interpretability to DNNs with very little compromise on performance.

Table 3: Accuracy of related work models in comparison to XNNT_{AB}. Blackbox models are marked as (×), partially interpretable models as (○), and fully interpretable models as (✓) models. Standard deviation for all experiments is at most 0.144 (on GE by T2G-Former), at least 0.000. Results for other models are taken from the respective papers, n.a. indicates that values are not available. Note: Related work models follow a different training pipeline than ours (see Sec. 4.2).

	AD ↑	CH ↑	CO ↑	GE ↑
× TabM	0.857	0.860	0.973	n.a
× TabR	0.870	0.862	0.976	n.a
× FT-Transformer	0.859	0.860	0.970	0.613
× NODE	0.857	0.858	n.a	0.539
× T2G-FORMER	0.859	0.862	n.a	0.655
○ TabNet	0.848	0.850	0.957	0.600
○ InterpreTabNet	0.874	n.a	n.a	n.a
✓ XNNT _{AB}	0.850	0.861	0.968	0.665

Table 3 shows accuracy of XNNT_{AB} in comparison to state-of-the-art neural models. Note that XNNT_{AB} is trained using 5-fold-cross-validation, while the other methods only use one split (with the data setup not reported in the literature) with 15 random

seeds (cf. Sec. 4.2). XNNTAB scores higher than TabNet on all datasets where results are available in the literature. On AD, XNNTAB performs comparably to TabM, NODE, FT-Transformer and T2G-FORMER and underperforms TabR and the partially interpretable InterpreTabNet. On CH, XNNTAB is comparable to all blackbox models. On CO, XNNTAB has lower performance than TabR and is comparable to the other blackbox models. On GE, XNNTAB outperforms all models under comparison. These results indicate that XNNTAB has little compromise on performance compared to the state-of-the-art while being interpretable, and can be an alternative to blackbox models.

5.2 Interpretability

A selection of rules extracted for the dictionary features on AD are shown in Table 4 and for SB in Table 5 (full list). The learned rules provide a global explanation of the model’s behavior (Figure 2), since the predictions are simply a linear combination of the learned features (rules). Each weight in this linear combination directly indicates whether the presence of the corresponding features increases or lowers the probability of a class, and to which extent.

Table 6 shows the average number of active features for each dataset. For CR, 19 out of the 57 features that we learn are active for the chosen p (70%). That means, one local explanation requires us to inspect 19 rules on average to understand the model’s prediction. However, that number decreases to 3 for SB with a threshold of $p = 80\%$. While the average number of active features varies for each dataset, the complexity of the rules is on average 2.4 for all datasets. That means, each rule is simple to understand, as it has approximately two conditions on average.

Table 4: A selection of dictionary features for the AD dataset. $|T_j|$ - size of the training subset that strongly activate feature j . Coverage of the rule reported as number of samples and percentage of samples. Table sorted by $|T_j|$.

j	$ T_j $	Description	Coverage
40	15294	marital_status_Married is False and educational_num < 13 and capital_gain <= 11625.0	8028.0
9	11968	marital_status_Married is False and age <= 37.5 and educational_num < 12	7271/0.61
8	11634	marital_status_Married is False and age <= 34.5 and educational_num < 12	6517/0.56
54	10889	marital_status_Married is False and age <= 31.5 and educational_num < 13	5953/0.55
44	7457	marital_status_Married is False and relationship_Not_in_family is False and age <= 25.5	3330/0.45
45	3975	marital_status_Married is False and age <= 22.5 and hours_per_week <= 32.5	1516/0.38
5	1758	age <= 20.5 and hours_per_week <= 24.5	754/0.43
34	1658	occupation_Other_service is False and capital_gain > 14682.0	547/0.33
26	1358	marital_status_Widowed and is False and capital_gain > 14682.0	546/0.40
50	982	age <= 72.0 and capital_gain > 15022.0	532/0.55
63	978	gender is Female and age <= 18.5 and hours_per_week <= 24.5	236/0.24
7	290	occupation_Farming_fishing is False and capital_gain > 19266.0 and hours_per_week > 27.5	209/0.73
18	226	relationship_Other_relative is False and capital_gain > 26532.0	185/0.82
22	225	occupation_Farming_fishing is False and capital_gain > 26532.0 and hours_per_week > 18.0	183/0.82
3	212	capital_gain > 34569.0	153/0.73

Table 5: Dictionary features for the SB dataset. $|T_j|$ - size of the training subset that strongly activate feature j . Coverage of the rule reported as number of samples and percentage of samples. Table sorted by $|T_j|$.

j	$ T_j $	Description	Coverage
5	2340	word_freq_edu \leq 0.125 and char_freq_21 $>$ 0.0645 and capital_run_length_longest $>$ 9.5	984/0.42
4	2240	word_freq_hp \leq 0.14998 and char_freq_24 $>$ 0.0119 and capital_run_length_longest $>$ 7.5	693/0.31
9	1415	word_freq_receive \leq 0.2249 and word_freq_hp $>$ 0.375 and char_freq_21 \leq 0.0659	465/0.33
2	1031	word_freq_hp \leq 0.6200 and char_freq_21 $>$ 0.0804 and char_freq_24 $>$ 0.0064	586/0.56
3	833	char_freq_21 $>$ 0.0775 and char_freq_24 $>$ 0.0595 and capital_run_length_longest $>$ 42.5	332/0.40

Table 6: Complexity of features on all datasets showing rule length (number of single terms in a rule), and active features per decision.

		AD	CH	CR	SB	CO	GE	CA
Rule Length	minimum	1	1	2	3	1	2	1
	average	2.18	1.8	2.9	3	2.2	2.8	2.2
	maximum	3	2	3	3	3	3	3
Active Features	minimum	23	19	13	1	89	25	21
	average	28.7	33	19	3.3	115	32	27
	maximum	34	40	23	5	137	40	35

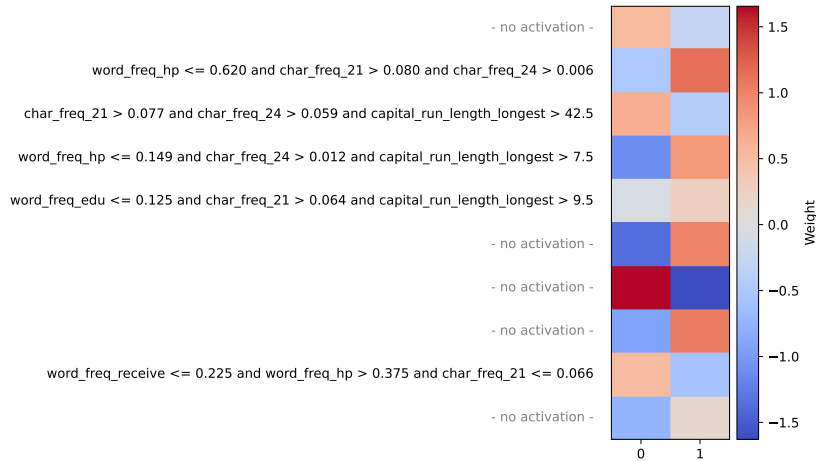
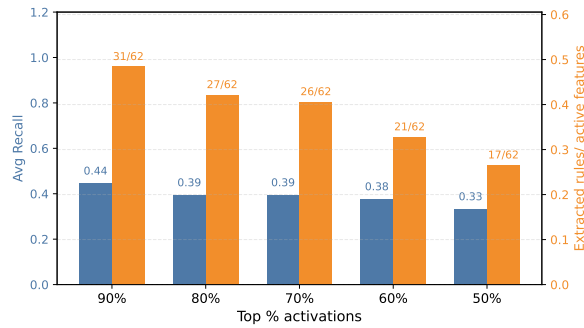


Fig. 2: Heatmap of decision weight matrix W' for SB on interpretable features.

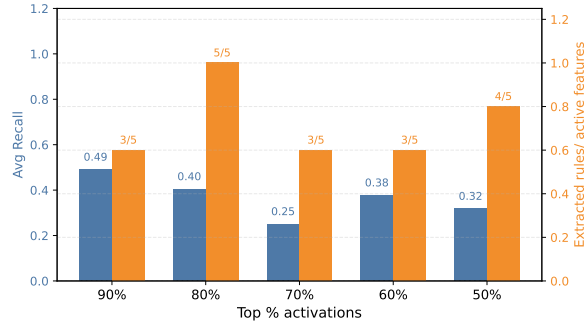
5.3 Ablation on Activation Threshold

The choice of p influences model interpretability in two ways. First, different p result in a different amount of features for which rules can be found, i.e., it defines the extent to which the model’s reasoning is explained. Second, different p result in different $|T_j|$, and therefore different recall values for the rules. The recall describes how many instances of $|T_j|$ are described by the rule and is therefore a measure of reliability.

Figure 3 shows for how many of the active features rules can be extracted, and the fraction of instances covered by rules (recall) for $p \in \{50\%, 60\%, 70\%, 80\%, 90\%\}$. On GE, lower p lead to fewer features being covered by Skope-rules, their average recall decreases accordingly. However, this behavior does not generalize over all datasets; for SB, both the number of extracted features and their respective average recall fluctuate as p decreases. Ultimately, choosing an optimal p for interpretability seems to depend on the dataset and requires to trade-off the number of covered features (i.e., the extent to which the model can be explained) and the average rule recall (i.e., reliability of a rule).



(a) GE dataset



(b) SB dataset

Fig. 3: Feature coverage on GE dataset (top) and SB dataset (bottom) for different p . **Orange bars** show the proportion of active features for which a rule was successfully extracted, **blue bars** show the average recall of the extracted rules.

6 Conclusion

In this paper, we introduce XNNT_{AB}, an interpretable model for tabular data. Our results show, that XNNT_{AB} outperforms interpretable models and performs comparably to blackbox architectures across several datasets, while being interpretable. By using a rule-based classifier, we show how the model’s output predictions can be explained by simple decision rules.

Although our model is interpretable, it has limitations: learning decision rules to explain learned features is post-hoc and not always complete, as it is not always possible to extract rules for all features. Furthermore, a high number of learned features results in a high average number of active features per prediction, which limits interpretability.

Directions for future work include investigating strategies to reduce redundant rules such as pruning or combining neurons, and exploring automated approaches for selecting activation thresholds that balance rule recall with the fraction of extracted rules. The SAE approach could also be extended to other blackbox neural models for tabular data to further enhance performance.

Acknowledgments. This work was funded by the Deutsche Forschungsgemeinschaft (DFG, German Research Foundation) under project ID 536124560.

A Implementation Details

A.1 Datasets

Standard preprocessing was applied to all datasets: removal of non-informative features (e.g. “RowNumber”, “CustomerId”), min-max normalization of numerical features, one hot encoding of nominal variables, and ordinal encoding of ordinal variables.

A.2 Hyperparameters

For all models, we use Optuna⁸ for hyperparameter tuning. We tune on the validation set of each split (5 splits in total). For each experiment, the number of iterations is set to 100. Random seed = 0.

RF. We tuned $n_estimators$ in [100, 200, 300], max_depth in [5, 10, 15, 20], $min_samples_split$ in [2, 10], and $min_samples_leaf$ in [1, 10].

XGBoost. We set the booster to *gbtree*, $early_stopping_rounds$ to 12, and tuned $learning_rate$ in [0.001, 0.4], max_depth in [3, 10], $subsample$ in [0.5, 1], λ in [0.1, 10]

DT. We tuned max_depth in [5, 10, 15, 20], $min_samples_split$ in [2, 10], and $min_samples_leaf$ in [1, 10].

LR. We tuned max_iter in [100, 200].

MLP. We tuned the learning rate (lr) in [$1e - 2$, $5e - 3$], $Dropout$ in [0.0, 0.5] and λ in [$1e - 7$, $1e - 2$] for L1 regularization.

XNNT_{AB}. Additional to the MLP parameters, SAE parameters are the L_1 coefficient $\alpha = 1e - 3$ for AD and CH.

Skope-rules. We set $precision_min = 1$, $recall_min = 0.2$, and used the default settings for the rest of the parameters.

⁸ <https://optuna.org>

Model Architectures:

- CH and AD: 3-layer base MLP (100, 64, 32); SAE with $2 \times 24 = 64$ (R=2) neurons.
- CR: 3-layer base MLP (174, 180, 19); SAE $3 \times 19 = 57$ (R=3) neurons.
- SB: 3-layer base MLP (96, 179, 5); SAE $2 \times 5 = 10$ (R=2) neurons.
- GE: 3-layer base MLP(128, 64, 32); SAE $2 \times 32 = 64$ (R=2) neurons.
- CO: 2-layer base MLP (169, 175), SAE $1 \times 175 = 175$ (R=1) neurons.
- CA: 2-layer base MLP (106, 44): the SAE $2 \times 44 = 88$ (R=2) neurons.

Bibliography

- [1] Akiba, T., Sano, S., Yanase, T., Ohta, T., Koyama, M.: Optuna: A next-generation hyperparameter optimization framework. In: Proceedings of the 25th ACM SIGKDD International Conference on Knowledge Discovery & Data Mining. p. 2623–2631. KDD '19, Association for Computing Machinery, New York, NY, USA (2019). <https://doi.org/10.1145/3292500.3330701>
- [2] Arik, S.Ö., Pfister, T.: TabNet: Attentive Interpretable Tabular Learning. Proceedings of the AAAI Conference on Artificial Intelligence **35**(8), 6679–6687 (May 2021). <https://doi.org/10.1609/aaai.v35i8.16826>
- [3] Blackard, J.A., Dean, D.J.: Comparative accuracies of artificial neural networks and discriminant analysis in predicting forest cover types from cartographic variables. Computers and Electronics in Agriculture **24**(3), 131–151 (1999). [https://doi.org/10.1016/S0168-1699\(99\)00046-0](https://doi.org/10.1016/S0168-1699(99)00046-0), <https://www.sciencedirect.com/science/article/pii/S0168169999000460>
- [4] Chen, J., Yan, J., Chen, Q., Chen, D.Z., Wu, J., Sun, J.: Can a Deep Learning Model be a *Sure Bet* for Tabular Prediction? In: Proceedings of the 30th ACM SIGKDD Conference on Knowledge Discovery and Data Mining. pp. 288–296. ACM, Barcelona Spain (Aug 2024). <https://doi.org/10.1145/3637528.3671893>
- [5] Chen, T., Guestrin, C.: XGBoost: A Scalable Tree Boosting System. In: Proceedings of the 22nd ACM SIGKDD International Conference on Knowledge Discovery and Data Mining. pp. 785–794. ACM, San Francisco California USA (Aug 2016). <https://doi.org/10.1145/2939672.2939785>
- [6] Elhadri, K., Michalski, T., Wróbel, A., Schlötterer, J., Zieliński, B., Seifert, C.: This looks like what? challenges and future research directions for part-prototype models (2025), <https://arxiv.org/abs/2502.09340>
- [7] Elhadri, K., Schlötterer, J., Seifert, C.: Towards interpretable deep neural networks for tabular data (2026), <https://arxiv.org/abs/2509.08617>
- [8] Gorishniy, Y., Kotelnikov, A., Babenko, A.: TabM: Advancing tabular deep learning with parameter-efficient ensembling. In: The Thirteenth International Conference on Learning Representations (Oct 2024)
- [9] Gorishniy, Y., Rubachev, I., Kartashev, N., Shlenskii, D., Kotelnikov, A., Babenko, A.: TabR: Tabular Deep Learning Meets Nearest Neighbors. In: The Twelfth International Conference on Learning Representations (Oct 2023)
- [10] Gorishniy, Y., Rubachev, I., Khrulkov, V., Babenko, A.: Revisiting deep learning models for tabular data. In: Proceedings of the 35th International Conference on Neural Information Processing Systems. NIPS '21, Curran Associates Inc., Red Hook, NY, USA (2021)
- [11] Grinsztajn, L., Oyallon, E., Varoquaux, G.: Why do tree-based models still outperform deep learning on typical tabular data? In: Proceedings of the 36th International Conference on Neural Information Processing Systems. pp. 507–520. NIPS '22, Curran Associates Inc., Red Hook, NY, USA (Nov 2022)

- [12] Huang, X., Khetan, A., Cvitkovic, M., Karnin, Z.: TabTransformer: Tabular Data Modeling Using Contextual Embeddings (Dec 2020). <https://doi.org/10.48550/arXiv.2012.06678>
- [13] Huben, R., Cunningham, H., Smith, L.R., Ewart, A., Sharkey, L.: Sparse Autoencoders Find Highly Interpretable Features in Language Models. In: The Twelfth International Conference on Learning Representations (Oct 2023)
- [14] Jeffares, A., Liu, T., Crabbé, J., Imrie, F., van der Schaar, M.: TANGOS: Regularizing Tabular Neural Networks through Gradient Orthogonalization and Specialization. In: The Eleventh International Conference on Learning Representations (Sep 2023)
- [15] Jiang, X., Margeloiu, A., Simidjievski, N., Jamnik, M.: ProtoGate: Prototype-based neural networks with global-to-local feature selection for tabular biomedical data. In: Proceedings of the 41st International Conference on Machine Learning. ICML'24, vol. 235, pp. 21844–21878. JMLR.org, Vienna, Austria (Jul 2024)
- [16] Khan, S., Naseer, M., Hayat, M., Zamir, S.W., Khan, F.S., Shah, M.: Transformers in Vision: A Survey. *ACM Comput. Surv.* **54**(10s), 200:1–200:41 (Sep 2022). <https://doi.org/10.1145/3505244>
- [17] Kohavi, R.: Scaling up the accuracy of naive-bayes classifiers: a decision-tree hybrid. In: Proceedings of the Second International Conference on Knowledge Discovery and Data Mining. p. 202–207. KDD'96, AAAI Press (1996)
- [18] Lee, K., Sim, Y.S., Cho, H.S., Eo, M., Yoon, S., Yoon, S., Lim, W.: Binning as a pretext task: Improving self-supervised learning in tabular domains. In: Proceedings of the 41st International Conference on Machine Learning. ICML'24, vol. 235, pp. 26929–26947. JMLR.org, Vienna, Austria (Jul 2024)
- [19] Madeo, R.C.B., Lima, C.A.M., Peres, S.M.: Gesture unit segmentation using support vector machines: segmenting gestures from rest positions. In: Proceedings of the 28th Annual ACM Symposium on Applied Computing. p. 46–52. SAC '13, Association for Computing Machinery, New York, NY, USA (2013). <https://doi.org/10.1145/2480362.2480373>
- [20] Popov, S., Morozov, S., Babenko, A.: Neural oblivious decision ensembles for deep learning on tabular data. In: International Conference on Learning Representations (ICLR) (2019)
- [21] Schwalbe, G., Finzel, B.: A comprehensive taxonomy for explainable artificial intelligence: A systematic survey of surveys on methods and concepts. *Data Mining and Knowledge Discovery* (2023). <https://doi.org/10.1007/s10618-022-00867-8>
- [22] Si, J., Cheng, W.Y., Cooper, M., Krishnan, R.G.: InterpreTabNet: Distilling predictive signals from tabular data by salient feature interpretation. In: Proceedings of the 41st International Conference on Machine Learning. ICML'24, vol. 235, pp. 45353–45405. JMLR.org, Vienna, Austria (Jul 2024)
- [23] Somepalli, G., Schwarzschild, A., Goldblum, M., Brass, C.B., Goldstein, T.: SAINT: Improved Neural Networks for Tabular Data via Row Attention and Contrastive Pre-Training. In: NeurIPS 2022 First Table Representation Workshop (Oct 2022)
- [24] Yan, J., Chen, J., Wu, Y., Chen, D.Z., Wu, J.: T2G-FORMER: Organizing tabular features into relation graphs promotes heterogeneous feature interaction. In:

Proceedings of the Thirty-Seventh AAAI Conference on Artificial Intelligence and Thirty-Fifth Conference on Innovative Applications of Artificial Intelligence and Thirteenth Symposium on Educational Advances in Artificial Intelligence. AAAI'23/IAAI'23/EAAI'23, vol. 37, pp. 10720–10728. AAAI Press (Feb 2023). <https://doi.org/10.1609/aaai.v37i9.26272>

- [25] Yun, Z., Chen, Y., Olshausen, B., LeCun, Y.: Transformer visualization via dictionary learning: contextualized embedding as a linear superposition of transformer factors. In: Agirre, E., Apidianaki, M., Vulić, I. (eds.) Proceedings of Deep Learning Inside Out (DeeLIO): The 2nd Workshop on Knowledge Extraction and Integration for Deep Learning Architectures. pp. 1–10. Association for Computational Linguistics, Online (Jun 2021). <https://doi.org/10.18653/v1/2021.deelio-1.1>, <https://aclanthology.org/2021.deelio-1.1/>